

RESEARCH PAPER

Green synthesis, characterization, photocatalytic and antibacterial activities of copper oxide nanoparticles

Saeid Taghavi Fardood^{1*}, Farzaneh Moradnia², Siamak Heidarzadeh³, Ali Naghipour¹

¹Department of Chemistry, Faculty of Science, Ilam University, Ilam, Iran

²Department of Chemistry, Faculty of Science, University of Zanjan, Zanjan, Iran

³Department of Microbiology and Virology, School of Medicine, Zanjan University of Medical Sciences, Zanjan, Iran

ARTICLE INFO

Article History:

Received 14 Feb 2023

Accepted 05 Mar 2023

Published 10 Mar 2023

Keywords:

Copper oxide

Green synthesis

Antibacterial activity

Photocatalytic activity

ABSTRACT

In this work, copper oxide nanoparticles were efficiently synthesized using a simple and environmentally friendly sol-gel process and their degradability of reactive blue 21 dye and antibacterial properties were studied. To characterize the synthesized CuO nanoparticles, powder X-ray diffraction (XRD), Brunauer Emmett Teller (BET), transmission electron microscope (TEM), field emission scanning electron microscopy (FESEM), and differential reflectance spectroscopy (DRS) analysis were employed. The particle size was determined using the TEM technique to be roughly 25 nm. The Tauc relation was used to calculate the optical band gap of CuO nanoparticles from the absorption spectra, which was found to be approximately 2.04 eV. The CuO NPs showed good photocatalysis activity towards the Reactive Blue 21 dye as an organic pollutant such that 86% of RB21 was removed in 60 min in room condition and visible light region. CuO NPs were evaluated for antibacterial efficacy against Gram negative (*Escherichia coli*, *Salmonella typhimurium*, *Proteus mirabilis*, *Pseudomonas aeruginosa*) and Gram positive (*Staphylococcus aureus*, *Enterococcus faecalis*) bacteria.

How to cite this article

Taghavi Fardood S., Moradnia F., Heidarzadeh S., Naghipour A., Green synthesis, characterization, photocatalytic and antibacterial activities of copper oxide nanoparticles. *Nanochem Res*, 2023; 8(2): 134-140 DOI: 10.22036/ncr.2023.02.006

INTRODUCTION

Physical, chemical, and environmentally friendly techniques have been utilized for the synthesis of nanoparticles. [1-5]. Recently, researchers focus on green synthesis techniques to prepare the various metal nanoparticles [6-10]. Metal oxide NPs and metal NPs have received great attention among other nanomaterials due to their promising properties [11, 12].

Industrial development and population expansion have led to increased environmental pollution which is a major global serious concern. Water pollution is a particularly pressing concern. Wastewater and water arriving from leather

industries paper, textiles, and plastic are usually rich in organic dyes. Degradation using photocatalysis is one of the significant and effective methods for water and wastewater treatment [13-16].

Research on nanoparticles and their use as antimicrobial agents has increased due to their unique physical-chemical properties in limiting bacterial growth [17]. Silver, gold [18], and Cu metal nanoparticles or oxides have been used in medicine, biology, and pharmacy in recent years [19]. Nanoparticles' antimicrobial action makes them useful in biology [20]. Previous research have shown that nanoparticles' antibacterial properties may change their structure, morphology, size, and functional group [21]. Instead, inorganic nanoparticles may be employed more after being

* Corresponding Author Email: s.taghavi@ilam.ac.ir
saeidt64@gmail.com



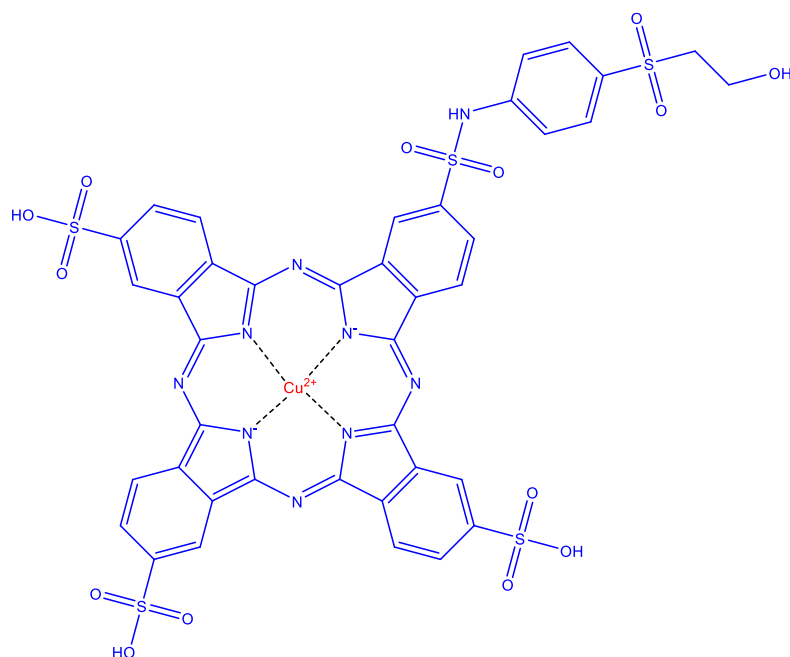


Fig. 1. Structure of Reactive blue 21 (RB21)

matched with organic nanoparticles owing to their stability and safety [22]. Metal oxide nanoparticles possess antibacterial properties against both gram-negative and gram-positive bacteria. This is attributed to their ability to bind to biological macromolecules, which inactivates them and leads to the death of bacteria, viruses, and fungi [23, 24]. Among metal oxide nanoparticles, CuO is a p-type semiconductor having electrochemical, catalytic, photocatalytic, and antibacterial capabilities [25–26]. Even at low concentrations, it has a significant antimicrobial impact against a broad spectrum of pathogens.

This study addressed the green sol-gel synthesis of CuO nanoparticles with photocatalytic and antibacterial activities. The photocatalytic activity of CuO NPs in aqueous solution was examined by degrading RB21 dye under visible light irradiation. In addition, the antibacterial activity of CuO NPs was assessed by measuring their minimum inhibitory and bactericidal concentrations (MIC and MBC) using broth microdilution. To analyze the produced nanoparticles, XRD, FESEM, TEM, BET, and DRS were employed. The molecular structure of the RB21 dye is shown in Fig. 1 [27].

EXPERIMENTAL

Materials

The tragacanth gum (TG) was acquired from a

bio shop. The $\text{Cu}(\text{NO}_3)_2 \cdot 3\text{H}_2\text{O}$ was acquired from Merck. CuO NPs were characterized by X-ray powder diffraction (XRD) utilizing Cu (K) radiation (wavelength: 1.5406 Å) on an X'Pert-PRO advanced diffractometer. UV–Vis absorption spectra were obtained on a Metrohm (Analytical Jena-Specord 205) double-beam. The diffuse reflectance UV–vis spectroscopy (DRS) of the sample was determined by a UV–Vis spectrophotometer (Shimadzu, UV-2550, Japan). BET method was applied to calculate the specific surface area of CuO (Belsorp Mini II apparatus). The morphology and size of the synthesized copper oxide were considered by the TEM (Philips CM30) and FESEM (Zeiss EVO 18, Germany).

Synthesis of Copper Oxide NPs

Firstly, tragacanth gum (TG) gel was prepared based on our previous work [28]. Then, 1.5 g of $\text{Cu}(\text{NO}_3)_2 \cdot 3\text{H}_2\text{O}$ salt was added to the prepared gel. The container was moved to a sand bath with the temperature stabilized at 75 °C for 12 h. Next, black color resin was calcined in air at 500 °C for 4 h to prepare copper oxide nanoparticles.

Photocatalytic experiment

All photocatalytic experiments were considered under the fluorescent. The rate of dye degradation was monitored in various conditions to determine

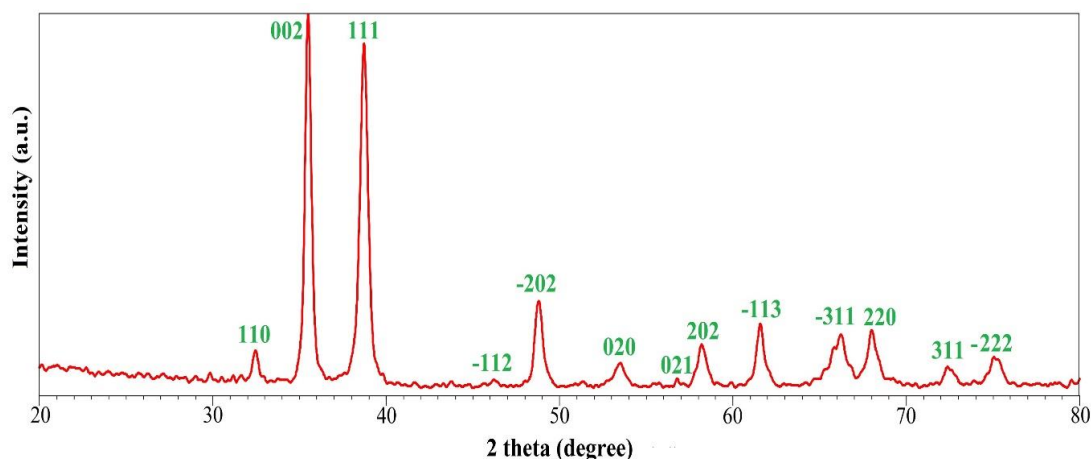


Fig. 2. XRD pattern of CuO NPs.

the impact of effective parameters. Thus, various amounts of copper oxide nanoparticles (0.02, 0.03, and 0.04) were applied in 50 ml of dye solution with different concentrations (10, 20, 30 mg/L). The degradation performance of reactive blue 21 dye was followed by UV-Vis at a $\lambda_{\text{max}} = 664 \text{ nm}$.

Antibacterial Activity of CuO Nanoparticles Bacterial Strains

Staphylococcus aureus ATCC 29213 (Gram-positive), *Enterococcus faecalis* ATCC 29212 (Gram-positive), *Escherichia coli* ATCC 25922 (Gram-negative), *Salmonella typhimurium* ATCC 14028 (Gram-negative), *Klebsiella pneumoniae* ATCC 7881 (Gram-negative), *Proteus mirabilis* ATCC 7002 (Gram-negative), and *Pseudomonas aeruginosa* ATCC 27853 (Gram-negative) were selected as bacterial models for evaluating the antimicrobial activity of CuO nanoparticles.

Minimum Inhibitory Concentration (MICs)

In order to evaluate the antibacterial susceptibility test of CuO nanoparticles, the MIC method (microdilution method) was applied. Initially, bacterial strains were grown separately in 5 ml of brain heart infusion (BHI) (Merck, Germany) at 37°C for 24 h. The bacterial suspension concentration was then adjusted to 0.5 McFarland standard ($1.5 \times 10^8 \text{ CFU/ml}$). Following, 200 μl of Mueller-Hinton broth (Merck, Germany) was added to each of the 96 microplate wells. In order to obtain a concentration in the range of 1-5 $\mu\text{g/ml}$, the stock concentration of CuO nanoparticles was diluted serially in 1% dimethyl sulfoxide (DMSO). After that, 100 μl of the prepared bacterial

suspension along with 100 μl of CuO were added to all microplate wells and incubated in a rotary shaker incubator (120 rpm) at 37°C for 18 h. The MIC was defined as the minimum concentration of CuO, resulting in no visible microbial growth after incubation period.

The minimum bactericidal concentration (MBC)

The MBC is the minimum concentration of an antimicrobial agent required to kill 99.9% of the bacteria, measured by subculturing the 50 μl of the broth dilutions applied for MIC determination on Mueller-Hinton agar (Merck, Germany) media and incubation for 18 h at 37°C. The absence of bacterial growth in the Mueller-Hinton agar medium is considered as MBC.

RESULTS AND DISCUSSION

Characterization of Copper Oxide NPs

Fig. 2 displays the X-ray diffraction patterns of the CuO NPs. Single-phase monoclinic structures were specified by the sharp and strong peaks. All diffraction peaks are indexed to the monoclinic structure of CuO (JCPDS card no. 80-1916). The crystallite size of the synthesized sample was calculated by the Scherrer formula [29] on the FWHM of the (002) diffraction peak and was obtained to be 21 nm.

The band gap of CuO NPs was calculated by UV-Vis DRS. The band gap energy was found by applying the Tauc model [30]. The results confirm that the band gap of copper oxide nanoparticles is 2.04 eV (Fig. 3). Therefore, the copper oxide NPs are appropriate photocatalyst in a visible-light region.

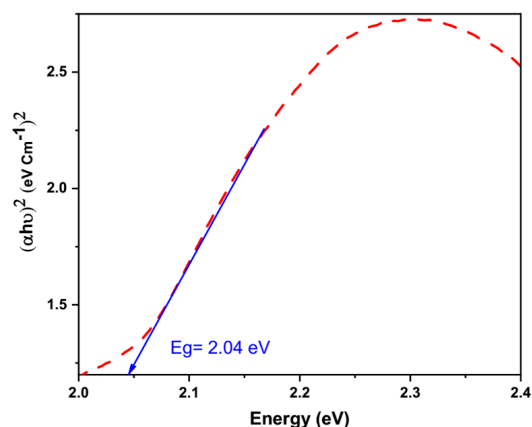


Fig. 3. Tauc plot of the CuO NPs.

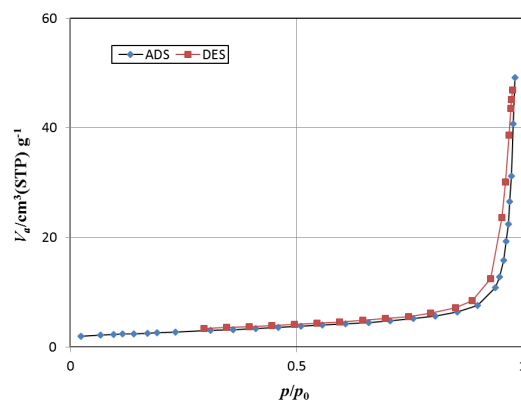
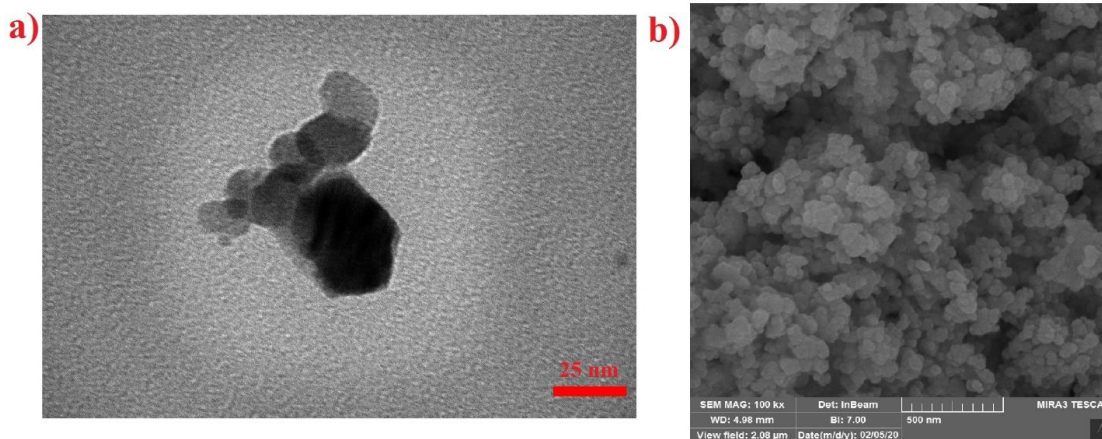
Fig. 4. The N_2 adsorption/desorption isotherm of the CuO NPs.

Fig. 5. a) TEM image and b) FESEM image of CuO NPs.

The specific surface area, pore diameter, and total pore volume of CuO NPs were specified *via* the BET technique, which were obtained to be $29.294 \text{ m}^2\text{g}^{-1}$, 32.726 nm and $0.076 \text{ cm}^3 \text{ g}^{-1}$, respectively. The nitrogen absorption/desorption curve of the sample was given in Fig 4. Isotherm is of type IV with hysteresis loops H1 based on the IUPAC classification of materials [31].

Fig. 5 shows the FESEM and TEM images of the CuO NPs synthesized by green sol-gel method. The images confirm the spherical shape of nanoparticles with a diameter of 25 nm.

Photocatalytic activity

Degradation of RB21 dye was done in three states to confirm the photocatalytic activity of CuO NPsL: visible light irradiation without CuO NPs (photolysis), nanoparticles under dark (adsorption), and CuO NPs under visible light irradiation (photocatalysis). For photolysis, adsorption, and

photocatalysis states, the degradation efficiencies are 2%, 45%, and 86%, respectively. These results indicate that synthesized copper oxide nanoparticles have the photocatalytic activity in the visible light region for RB21 degradation (Fig. 6a). To find the best amount of photocatalyst, 0.02-0.04 g of the CuO NPs was added in RB21 solution (50 ml, 20 mg/L), at a fixed time of 60 min (Fig. 6b). It is obvious that raising the catalyst dosage leads to an improvement in the degrading performance. The initial dye concentration is the significant parameter that affected the degradation efficiency [32]. Thus, the photocatalytic degradation of RB21 dye was monitored by varying the RB21 concentrations (10-30 mg/L) with the optimum dosage of CuO (0.03 g). As given in Fig. 6c, the decolorization performance of RB21 dye is reduced by increasing the dye concentration from 20 to 30 mg/L. Then, UV-Vis absorbance spectra of selected dye were monitored in different time periods

Table 1. MIC and MBC of CuO nanoparticles against a range of pathogenic bacteria

Organism	ATCC	Types of bacteria	MIC of CuO ($\mu\text{g/mL}$)	MBC of CuO ($\mu\text{g/mL}$)	Control (1% DMSO)
<i>Salmonella typhimurium</i>	14028	Gram-negative	1	1.25	not active
<i>Escherichia coli</i>	25922	Gram-negative	1	1.25	not active
<i>Pseudomonas aeruginosa</i>	27853	Gram-negative	1.5	2	not active
<i>Proteus mirabilis</i>	7002	Gram-negative	1	1.25	not active
<i>Klebsiella pneumoniae</i>	7881	Gram-negative	1	1.25	not active
<i>Enterococcus faecalis</i>	29212	Gram-positive	1	1	not active
<i>Staphylococcus aureus</i>	29213	Gram-positive	1	1	not active

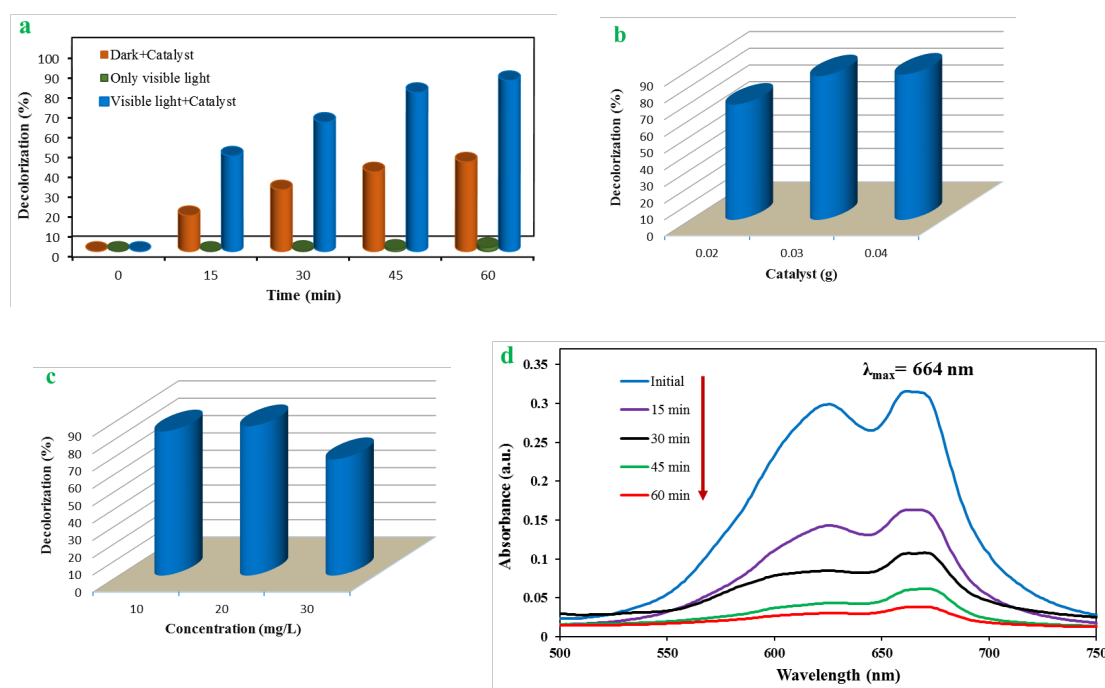


Fig. 6 a) Effect of visible light irradiation b) the effect of photocatalyst dosage c) Effect of initial concentration d) Absorption spectra of RB21 solutions under visible light radiation

to examine the impact of irradiation time on decolorization efficiency. Significant decreases in absorbance intensity at 664 nm (λ_{max} of RB21 dye) with increasing the irradiation time are shown in Fig. 6d. Based on the results, 86% of RB21 dye was removed in 60 min.

Antibacterial activity

MIC Results: All of the bacteria studied, including *S. aureus*, *E. faecalis*, *S. typhimurium*, *K. pneumoniae*, *P. mirabilis*, and *E. coli*, were significantly inhibited by CuO nanoparticles.

However, *P. aeruginosa* (1.5 $\mu\text{g/mL}$) were moderately inhibited by CuO (Table 1).

MBC Results: The highest MBC of CuO was found against gram-positive bacteria, *E. faecalis* and *S. aureus* (1 $\mu\text{g/mL}$). MBC of CuO against *S. typhimurium*, *K. pneumoniae*, *P. mirabilis*, and *E. coli* was 1.25 $\mu\text{g/mL}$. However, the lowest MBC was observed against *P. aeruginosa* (2 $\mu\text{g/mL}$) (Table 1).

CONCLUSION

This research examined the green synthesis of CuO nanoparticles with photocatalytic and

antibacterial applications. The sample were studied by XRD, FESEM, BET, DRS, and TEM techniques. The XRD and FESEM results verified their spherical shape and nano-crystallite size. The bandgap energy of CuO-NPs was found to be 2.04 eV. The photocatalytic results confirmed the photocatalyst function of CuO NPs during the whole RB 21 degradation process under visible light irradiation, with an obtained 86% degradation rate. The CuO nanoparticles demonstrated a significant antibacterial effect against both gram-negative and positive bacteria. According to the results of this study and other previous studies, it can be concluded that these nanoparticles can be used in the treatment of multidrug-resistant bacteria in the future.

ACKNOWLEDGMENT

The authors would like to appreciate “*Ilam University*”.

CONFLICT OF INTEREST

The authors declare no conflicts of interest.

REFERENCES

1. Taghavi Fardood S, Ramazani A, Joo SW. Journal of Applied Chemical Research. Eco-friendly Synthesis of Magnesium Oxide Nanoparticles using Arabic Gum. 2018;12(1):8-15.
2. Bangale SV, Bamane SR. Preparation and electrical properties of nanostructured spinel $ZnCr_2O_4$ by combustion route. Journal of Materials Science: Materials in Electronics. 2013;24(1):277-81. <https://doi.org/10.1007/s10854-012-0739-0>
3. Abirami M, Kannabiran K. Streptomyces ghanaensis VITHM1 mediated green synthesis of silver nanoparticles: Mechanism and biological applications. Frontiers of Chemical Science and Engineering. 2016;10(4):542-51. <https://doi.org/10.1007/s11705-016-1599-6>
4. Yu ZJ, Rajesh Kumar M, Wu QY, Chu Y, Sha K, Xie HD. Effect of Mn-doping on the structural, optical, and magnetic properties of ZnO nanoparticles by chemical method. Materials Research Express. 2017;4(2):025017. <https://doi.org/10.1088/2053-1591/aa5857>
5. Bo L, Xiaoyun L, Canfeng Z, Xiaoying W, Runcang S. Facile and green synthesis of silver nanoparticles in quaternized carboxymethylchitosan solution. Nanotechnology. 2013;24 (23):235601. <https://doi.org/10.1088/0957-4484/24/23/235601>
6. Atrak K, Ramazani A, Taghavi Fardood S. Green synthesis of $Zn_{0.5}Ni_{0.5}AlFeO_4$ magnetic nanoparticles and investigation of their photocatalytic activity for degradation of reactive blue 21 dye. Environmental Technology. 2020;41(21):2760-70. <https://doi.org/10.1080/09593330.2019.1581841>
7. Wen S, Yang T, Zhao N, Ma L, Liu E. Ni-Co-Mo-O nanosheets decorated with NiCo nanoparticles as advanced electrocatalysts for highly efficient hydrogen evolution. Applied Catalysis B: Environmental. 2019;258:117953. <https://doi.org/10.1016/j.apcatb.2019.117953>
8. Taghavi Fardood S, Moradnia F, Moradi S, Foroootan R, Yekke Zare F, Heidari M. Eco-friendly synthesis and characterization of $\alpha-Fe_2O_3$ nanoparticles and study of their photocatalytic activity for degradation of Congo red dye. Nanochemistry Research. 2019;4(2):140-7.
9. Wasilewska A, Klekotka U, Zambrzycka M, Zambrowski G, Świącicka I, Kalska-Szostko B. Physico-chemical properties and antimicrobial activity of silver nanoparticles fabricated by green synthesis. Food Chemistry. 2023;400:133960. <https://doi.org/10.1016/j.foodchem.2022.133960>
10. Singh C, Anand SK, Upadhyay R, Pandey N, Kumar P, Singh D, et al. Green synthesis of silver nanoparticles by root extract of *Premna integrifolia* L. and evaluation of its cytotoxic and antibacterial activity. Materials Chemistry and Physics. 2023;297:127413. <https://doi.org/10.1016/j.matchemphys.2023.127413>
11. Jeevanandam J, Kiew S, Ansah S, Sie Yon JL, Barhoum A, Danquah M, et al. Green approaches for the synthesis of metal and metal oxide nanoparticles using microbial and plant extracts. Nanoscale. 2022;14. <https://doi.org/10.1039/D1NR08144F>
12. Kumar U, Hassan JZ, Bhatti RA, Raza A, Nazir G, Nabgan W, et al. Photocatalysis vs adsorption by metal oxide nanoparticles. Journal of Materials Science & Technology. 2022;131:122-66. <https://doi.org/10.1016/j.jmst.2022.05.020>
13. Zhao L, Li X, Zhao J. Fabrication, characterization and photocatalytic activity of cubic-like $ZnMn_2O_4$. Applied Surface Science. 2013;268:274-7. <https://doi.org/10.1016/j.apsusc.2012.12.078>
14. Menaka, Qamar M, Lofland SE, Ramanujachary KV, Ganguli AK. Magnetic and photocatalytic properties of nanocrystalline $ZnMn_2O_4$. Bulletin of Materials Science. 2009;32(3):231-7. <https://doi.org/10.1007/s12034-009-0035-7>
15. Ahmadi F, Rahimi-Nasrabadi M, Behpour M. Synthesis Nd_2TiO_5 nanoparticles with different morphologies by novel approach and its photocatalyst application. Journal of Materials Science: Materials in Electronics. 2017;28(2):1531-6. <https://doi.org/10.1007/s10854-016-5692-x>
16. Abbas N, Shao GN, Imran SM, Haider MS, Kim HT. Inexpensive synthesis of a high-performance $Fe_3O_4-SiO_2-TiO_2$ photocatalyst: Magnetic recovery and reuse. Frontiers of Chemical Science and Engineering. 2016;10(3):405-16. <https://doi.org/10.1007/s11705-016-1579-x>
17. Karunakaran C, Rajeswari V, Gomathisankar P. Enhanced photocatalytic and antibacterial activities of sol-gel synthesized ZnO and Ag-ZnO. Materials Science in Semiconductor Processing. 2011;14(2):133-8. <https://doi.org/10.1016/j.mssp.2011.01.017>
18. Nguyen THA, Nguyen V-C, Phan TNH, Le VT, Vasseghian Y, Trubitsyn MA, et al. Novel biogenic silver and gold nanoparticles for multifunctional applications: Green synthesis, catalytic and antibacterial activity, and colorimetric detection of Fe(III) ions. Chemosphere. 2022;287:132271. <https://doi.org/10.1016/j.chemosphere.2021.132271>
19. Rasool A, Kanagaraj T, Mir MI, Zulfajri M, Ponnusamy VK, Mahboob M. Green coalescence of CuO nanospheres for efficient anti-microbial and anti-cancer conceivable activity. Biochemical Engineering Journal. 2022;187:108464. <https://doi.org/10.1016/j.bej.2022.108464>
20. Iqbal H, Fatima A, Khan HAA. ZnO nanoparticles produced in the culture supernatant of *Bacillus thuringiensis* ser. israelensis affect the demographic parameters of

- Musca domestica using the age-stage, two-sex life table. *Pest Management Science*. 2022;78(4):1640-8. <https://doi.org/10.1002/ps.6783>
21. Babayevska N, Przysiecka Ł, Iatsunskiy I, Nowaczyk G, Jarek M, Janiszewska E, et al. ZnO size and shape effect on antibacterial activity and cytotoxicity profile. *Scientific Reports*. 2022;12(1):8148. <https://doi.org/10.1038/s41598-022-12134-3>
 22. Gudkov SV, Burmistrov DE, Smirnova VV, Semenova AA, Lisitsyn AB. A Mini Review of Antibacterial Properties of Al₂O₃ Nanoparticles. *Nanomaterials* [Internet]. 2022; 12(15). <https://doi.org/10.3390/nano12152635>
 23. Pachaiappan R, Rajendran S, Show PL, Manavalan K, Naushad M. Metal/metal oxide nanocomposites for bactericidal effect: A review. *Chemosphere*. 2021;272:128607. <https://doi.org/10.1016/j.chemosphere.2020.128607>
 24. Naseem T, Durrani T. The role of some important metal oxide nanoparticles for wastewater and antibacterial applications: A review. *Environmental Chemistry and Ecotoxicology*. 2021;3:59-75. <https://doi.org/10.1016/j.enceco.2020.12.001>
 25. Leneff JD, Jo J, Trejo O, Mandia DJ, Peterson RL, Dasgupta NP. Plasma-Enhanced Atomic Layer Deposition of p-Type Copper Oxide Semiconductors with Tunable Phase, Oxidation State, and Morphology. *The Journal of Physical Chemistry C*. 2021;125(17):9383-90. <https://doi.org/10.1021/acs.jpcc.1c00429>
 26. Taghavi Fardood S, Ramazani A. Black Tea Extract Mediated Green Synthesis of Copper Oxide Nanoparticles. *Journal of Applied Chemical Research*. 2018;12(2):8-15
 27. Moradnia F, Ramazani A, Taghavi Fardood S, Gouranlou F. A novel green synthesis and characterization of tetragonal-spinel MgMn₂O₄ nanoparticles by tragacanth gel and studies of its photocatalytic activity for degradation of reactive blue 21 dye under visible light. *Materials Research Express*. 2019;6(7):075057. <https://doi.org/10.1088/2053-1591/ab17bc>
 28. Taghavi Fardood S, Ramazani A, Joo SW. Green Chemistry Approach for the Synthesis of Copper Oxide Nanoparticles Using Tragacanth Gel and Their Structural Characterization. *Journal of Structural Chemistry*. 2018;59(2):482-6. <https://doi.org/10.1134/S0022476618020324>
 29. Taghavi Fardood S, Moradnia F, Ramazani A. Green synthesis and characterisation of ZnMn₂O₄ nanoparticles for photocatalytic degradation of Congo red dye and kinetic study. *Micro & Nano Letters*. 2019;14(9):986-91. <https://doi.org/10.1049/mnl.2019.0071>
 30. Taghavi Fardood S, Foroootan R, Moradnia F, Afshari Z, Ramazani A. Green synthesis, characterization, and photocatalytic activity of cobalt chromite spinel nanoparticles. *Materials Research Express*. 2020;7(1):015086. <https://doi.org/10.1088/2053-1591/ab6c8d>
 31. Sing KSW. Reporting physisorption data for gas/solid systems with special reference to the determination of surface area and porosity (Provisional). 1982;54(11):2201-18. <https://doi.org/10.1351/pac198254112201>
 32. Moradi S, Taghavi Fardood S, Ramazani A. Green synthesis and characterization of magnetic NiFe₂O₄@ZnO nanocomposite and its application for photocatalytic degradation of organic dyes. *Journal of Materials Science: Materials in Electronics*. 2018;29(16):14151-60. <https://doi.org/10.1007/s10854-018-9548-4>